On the correlation between thermal analysis results and corrosion behaviour of some metallic religious artefacts

Iulian Rusu · Daniel Sutiman · Gabriela Lisa · Daniel Mareci · Nicoleta Melniciuc Puică

Abstract The aim of this study was to investigate the effects of immersion time on the electrochemical corrosion behaviour of three brass alloys (CuZn) coming from religious artefacts in simulated acid rain at 25 °C, utilising the electrochemical impedance spectroscopy (EIS). The main parameters of the corrosion process were established. On the other hand, the alloys were also analysed by means DSC and TG/DTA before and after immersion in the corrosive environment. Finally, the obtained results were compared in order to correlate them with each other and with the corrosion process.

Keywords Alloys · Acid passivation · Oxidation · Decomposition

Introduction

For the conservation–restoration field, a pollutant is defined as any reactive chemical compound in a gaseous, liquid or particulate state found in the preservation environmental of art objects. These agents of deterioration may interact with the materials of objects and artefacts in ways that greatly accelerate their deterioration. It is difficult to identify the lowest level of pollutants as which damage to materials can occur, because the often synergistic effect of environmental pollutants, relative humidity and the extreme variability of materials housed in collections. Corrosion develops under thin layers of adsorbed oxygen and water and only a few adsorbed molecular layers of moisture are required for corrosion to proceed [1].

In recent years, the susceptibility of Fe, Cu, Ag and bronze, as constituent materials of art object, to corrosion due pollutant agents were referenced as well [2–5]. However, the complicate nature of interaction between pollutants and their ability to enhance the deterioration or corrosion process is not completely understood.

By rapid electrochemical tests we can monitor the samples, at least in the qualitative way, with respect to their corrosion resistance.

The electrochemical methods based on the open circuit potential and polarisation curves recording are frequently used. Direct current (DC) electrochemical methods are commonly used to evaluate corrosion, but over the past decade many articles on the electrode impedance spectroscopy (EIS) have been published and was demonstrated that the alternative current (AC) impedance method is particularly useful when monitoring some electrochemical changes as a function of time, being a non-destructive technique [6–9].

On the other hand, thermal analysis can provide useful information on the behaviour of alloys [10]. Consequently, our study is dealing with the corrosion of three brass alloys (CuZn) coming from religious artefacts and the possible correlation of the obtained data with those coming from thermal analysis.

I. Rusu (✉) · D. Sutiman · G. Lisa · D. Mareci
Department of Chemical Engineering, Faculty of Chemical Engineering and Environmental Protection, Technical University of Iasi, 71 D. Mangeron Blvd., 700050 Iasi, Romania
e-mail: rusu_iulian@hotmail.com

N. M. Puică
Faculty of Orthodox Theology, University 'Al. I. Cuza', 9 Closca, 700065 Iasi, Romania

Experimental

The analysed brass alloys have the compositions presented in Table 1. The solution of simulated acid rain was prepared according to literature [11].

Electrochemical measurements were carried out at 25 ± 1 °C. The working electrode, processed in cylindrical shape and mounted in a tetrafluoroethylene support, presents a one-dimensional circular area surface exposed to corrosion.

The sample was cut to 1.9 cm^2 size and the brass nut was attached to each sample using conductive paint to ensure electrical conductivity. The assembly was then embedded into an epoxy resin disk. Then, the sample was ground with SiC abrasive paper up to 2000 grit, while the final polishing was done with 1 μm alumina suspension. The sample was degreased with ethyl alcohol followed by ultrasonic cleaning with deionised water and dried under a hot air stream.

The electrochemical measurements were made with a potentiostatic assembly of three electrodes: a working electrode, a platinum counter-electrode and a reference electrode of saturated calomel (SCE). All potentials referred in this article are with respect to SCE. The measurement system was managed by a VoltaLab 40 potentiostat controlled by a personal computer with dedicated software (VoltaMaster 4).

Electrochemical impedance spectroscopy (EIS) was used to evaluate the corrosion resistance of the samples. The EIS spectra were obtained at 1 min, 1 h and 1 day after the electrode was immersed in the solutions. The alternating current (AC) impedance spectra for brass alloys were obtained, with a scan frequency range of 100 kHz to 10 mHz with amplitude of 10 mV. In order to supply quantitative support for discussions of these experimental EIS results, an appropriate model (Convertor-Radiometer, France and ZSimpWin-PAR, USA) for equivalent circuit (EC) quantification has also been used.

The surfaces of brass alloys were investigated using a Vega Tescan scanning electron microscope (model VEGA II LMH) having detector (model xflash, Bruker) for EDX analysis.

XRD spectra were recorded using an X'Pert PRO MRD, PANalytical Holland diffractometer and Cu K$_\alpha$ radiation.

Table 1 Chemical composition of the investigated brass samples

	Composition/wt%
Samples 1	Cu: 63, Zn: 37
Samples 2	Cu: 61, Zn: 36, In: 3
Samples 3	Cu: 57, Zn: 32, Ni: 11

Corroded and uncorroded samples of about 150–200 mg were submitted to both to DSC and TG/DTA analyses.

The air supplied by a compressor (4–5 bar) was passed over granular silica gel. The nitrogen was supplied from Linde gas cylinder (150 bar) of 4.6 purity class (99.996%). Thermogravimetric analyses (TG and DTA) were performed under nitrogen or air flow (20 cm^3 min^{-1}) at a heating rate of 10 °C/min from 25 to 1000 °C with a *Mettler Toledo model TGA/SDTA 851*.

DSC analysis was performed using a Mettler Toledo DSC 1 (Mettler Toledo, Switzerland) operating with version 9.1 of Stare software. The samples were encapsulated in aluminium pans having pierced lids to allow escape of volatiles. The heating rates of 5, 10 and 15 °C min^{-1}, from 25 to 400 °C and nitrogen purge at 120 mL min^{-1} were employed. In order to observe phase transitions, one sample was submitted to a cycle: heating–cooling–heating in the range of 25 to 400 °C.

Results and discussion

The variation of open circuit potential with times on immersion in simulated acid rain is the same for all brass alloys. The potential moved towards noble potentials on immersion. In all cases, the change of open circuit potential with time is accompanied by the formation of a film of corrosion products seen by visual inspection. It is likely that the main constituent of the film is cooper oxide.

The EIS spectra are shown in Bode plots of the logarithm of the impedance magnitude and of the phase angle as function of the logarithm of the frequency. Bode plots of all three brass alloys immersed for 1 min, 1 h and 1 day in simulated acid rain are shown in Fig. 1.

For the interpretation of the electrochemical behaviour of a system from EIS spectra, an appropriate physical model of the electrochemical reactions occurring on the electrodes is necessary. The electrochemical cell, because it presents impedance to a small sinusoidal excitation, may be represented by an equivalent circuit (EC). An EC consists of various arrangements of resistances, capacitors and other circuit elements, and provides the most relevant corrosion parameters applicable to the substrate/electrolyte system. The fitting quality of EIS data was estimated by both the chi-square (χ^2) test between (10^{-5} and 5×10^{-4}) values and the comparison between error distribution versus frequency values ($\pm 2\%$ for the whole frequency range) corresponding to experimental and simulated data. The phase angle plots (Fig. 1) reveal only one peak for all brass alloys immersed for 1 min in simulated acid rain, indicating the involvement of a single time constant. In this case, the simple EC consisting of only one time constant (Fig. 2a) was used to model the experimental impedance
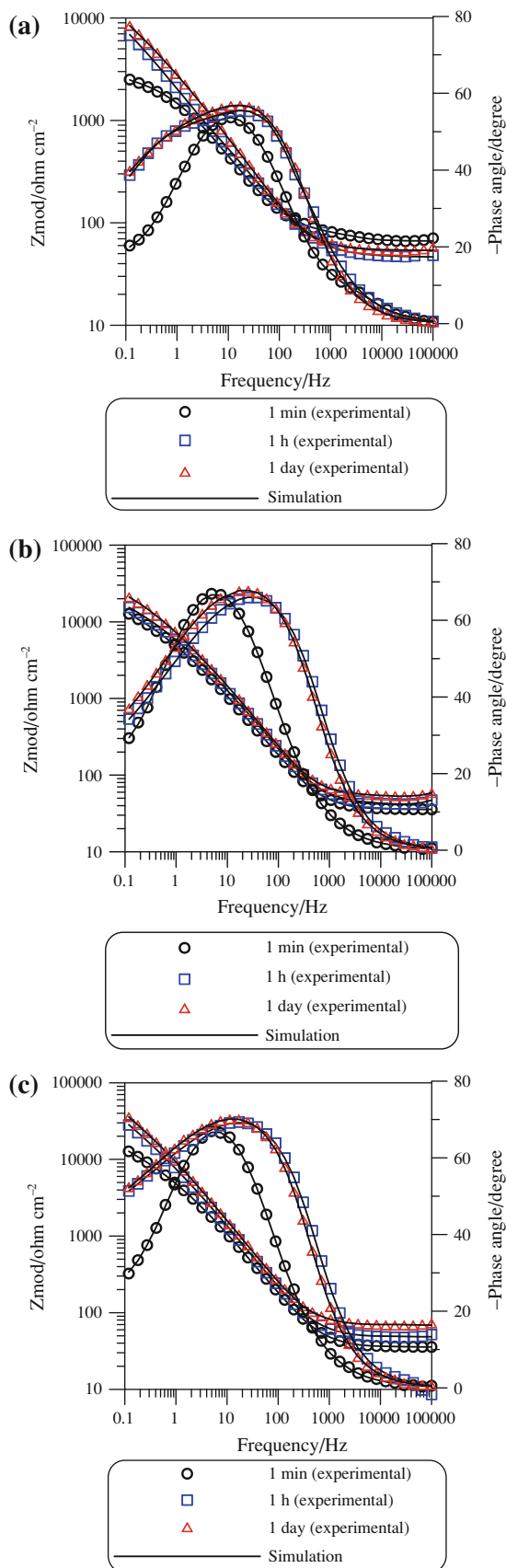
Fig. 1 Bode plots recorded at open circuit potential after immersion for 1 min, 1 h and 1 day in simulated acid rain: **a** sample 1, **b** sample 2 and **c** sample 3
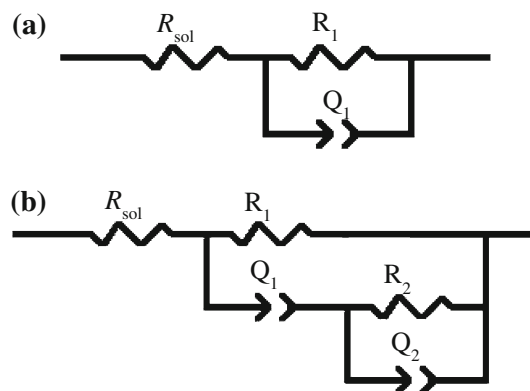
Fig. 2 Equivalent circuits (EC) used to fit the impedance data

spectra and the resultant EIS parameters are given in Table 2. A very good agreement between the experimental data and fitted data was obtained. The value of R₁ representing the charge transfer resistance (R_{ct}) is quite low (order of $10^3 \ \Omega \ cm^2$) and indicates the low stability of brass alloys after 1 min immersion in simulated acid rain. Charge transfer resistance (R_{ct}) is defined generally for kinetically controlled electrochemical reaction. The element Q₁ represents the double layer capacitance (C_{dl}) as shown by the high value of the n_1 exponent (around 0.85). The impedance spectra fitting for brass alloys after 1 h and 1 day immersion in simulated acid rain was carried out with an EC (Fig. 2b) using a series combination of the R_{sol} solution resistance, with two RQ elements in parallel: $R_{sol}(Q_1(R_1(R_2Q_2)))$.

Although from examination of these spectra in Fig. 1a–c it appears that the equivalent circuit requires only one RQ, the quality of the fit is improved, and associated errors are reduced, if the second RQ is introduced. The values of chi-square (χ^2) test for $R_{sol}(R_1Q_1)$ model were about 10^{-2}. The two RQ elements can be attributed to charge transfer at the metal-oxide film interface and to the oxide layer formed on the surface.

The oxide layer formed on the surface was confirmed by XRD test. Figure 3 shows the XRD pattern of the sample 1 after immersion for 1 day in simulated acid rain. The Cu_2O, CuO and ZnO compounds can be observed in these patterns.

The same value for cell resistance, R_{sol}, equals $45 \pm 5 \ \Omega$, was observed for all of the specimens regardless of the time of immersion and it was not inserted in Table 2.

Table 2 Impedance parameters for brass alloys in simulated acid rain at open circuit potential

	R_1/kΩ cm^2	10^5 Q_1/S cm^{-2} s^n	n_1	R_2/kΩ cm^2	10^5 Q_2/S cm^{-2} s^n	n_2
The samples maintained for 1 min in test solution						
Sample 1	4.6	2.2	0.84	–	–	–
Sample 2	7.9	1.9	0.85	–	–	–
Sample 3	8.4	1.5	0.85	–	–	–
The samples maintained for 1 h in test solution						
Sample 1	1.1	1.1	0.86	8.5	2.9	0.65
Sample 2	1.1	1.3	0.87	19	2.6	0.68
Sample 3	1.2	1.2	0.87	22	2.5	0.71
The samples maintained for 1 day in test solution						
Sample 1	1.2	1.2	0.87	9.8	1.9	0.67
Sample 2	1.2	1.2	0.87	22	2.3	0.71
Sample 3	1.2	1.1	0.88	34	2.3	0.71
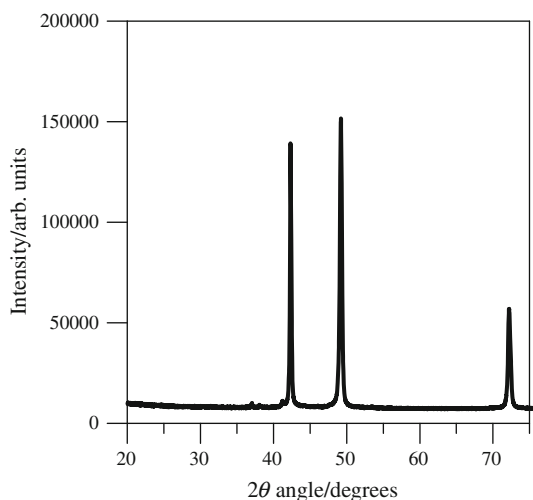
Fig. 3 XRD pattern of sample 1 immersed 1 day in simulated acid rain

In Fig. 1, the experimental data are shown as individual points, while the theoretical spectra resulting from the fits to a relevant EC model are shown as lines.

The overall polarisation resistance R_p is represented by the sum of partial resistance ($R_1 + R_2$) [12]. R_p allows a quantitative analysis based on the specific magnitudes of the corrosion rate. A high value is an indication of the working electrode strongly resisting change from its equilibrium state and is representative of the degree of protection of the passivation layer of the alloy surface. The more the value of R_p increases, the more the alloy will resist corrosion.

The polarisation resistance for all brass alloys increases with time after 1 h of immersion. This phenomenon must be associated with the formation of the protective oxide film on the surface of all the samples. For the brass alloys after 1 h and 1 day of immersion in simulated acid rain, the values of n_2 are small in the range of 0.65–0.7 indicating the presence of a diffusion process within the interfacial layer of the solution.

Such a diffusion process indicates a reversible dissolution process; i.e. the oxide film formation under open circuit condition proceeds through a dissolution–precipitation mechanism [13].

The oxide film presents a protective character and the polarisation resistance increases with the immersion time, probably because the oxidation kinetics process is diffusion controlled associated to mass transport of the ions inside the film pores. The corrosion resistance of the three brass alloys decreases in the following order: sample 3 > sample 2 > sample 1. No effective protection against corrosion was achieved by all the samples, as the passive oxide film formed on the brass alloy cannot effectively isolate the alloy from the aggressive environment. These aspects results in absolute values of the impedance around 10^4 Ω cm^2.

The analysis of SEM analyses (Fig. 4) indicates the appearance of corrosion points at the surface of sample 2, and the development of a uniform corrosion process in case of sample 1 and sample 3.

In this article, we used conventional differential scanning calorimetry (DSC) to determine the reaction kinetics using nth order kinetics. The nth order kinetics allow calculating the activation energy (E_a), pre-exponential factor (k_0) and reaction order (n) from a single DSC scan and the equation:

$$\frac{d\alpha}{dt} = k_0 e^{-\frac{E_a}{RT}} (1 - \alpha)^n \tag{1}$$

were $d\alpha/dt$—rate of reaction in s^{-1}, k_0—pre-exponential factor, E_a—activation energy in J mol^{-1}, R—gas constant = 8.31 J mol^{-1} K^{-1}, sample temperature in K, α—conversion of reaction and n—order of reaction [14].
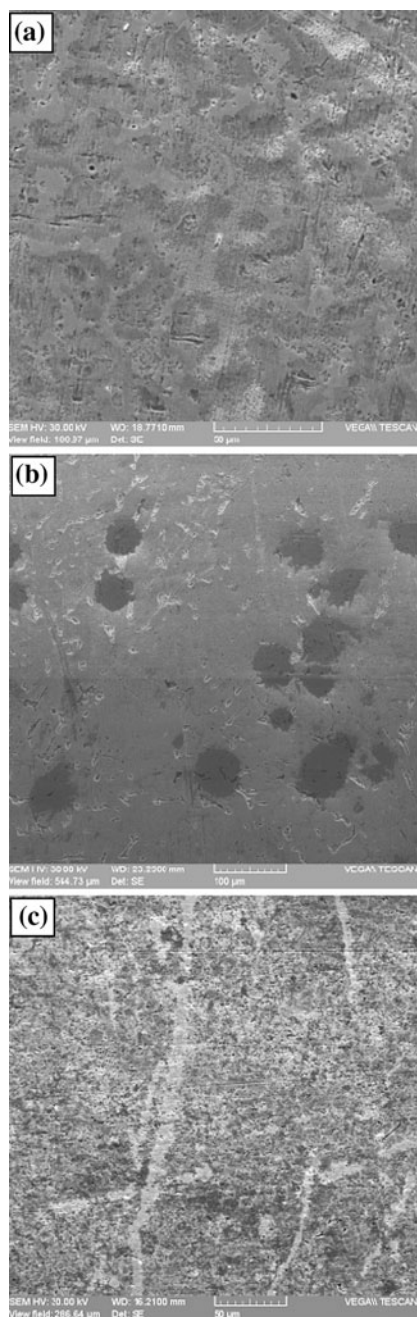
Fig. 4 SEM observations of: **a** sample 1, **b** sample 2 and **c** sample 3 after 1 day of immersion in simulated acid rain

Table 3 DSC characteristic temperatures and thermal effects of the studied alloys

Sample	Heating rate/ °C min^{-1}	T_i/°C	T_p/°C	T_f/°C	ΔQ/J g^{-1}
Sample 2 (heating)	5	314.82	319.48	322.59	−0.51
	10	314.55	319.98	325.35	−0.49
	15	313.92	319.79	326.81	−0.72
Sample 2 (cooling)	5	302.57	294.74	287.78	0.42
	10	302.21	294.27	284.15	0.41
	15	303.49	294.09	280.44	0.55
Sample 2 (re-heating)	5	314.99	319.49	322.45	−0.55
	10	314.67	319.72	325.24	−0.59
	15	314.16	319.80	326.86	−0.69
Sample 3 (heating)	5	317.67	323.78	326.01	−0.0053
	10	319.68	323.86	327.06	−0.0040
	15	319.84	324.04	328.04	−0.0032

In Tables 3 and 4 are listed the characteristic temperatures (initial—T_i, peak—T_p and final—T_f), the thermal effects and the kinetic parameters obtained by means of DSC analyses. Sample 1 presented no obvious thermal effect.

As can be observed from Table 3 for both samples 2 and 3 appears a phase transformation in almost the same temperature region. The main difference concerns the value of the thermal effect which is much larger for sample 2. On the other hand, taking into account the characteristic temperatures, the thermal effects and the kinetic parameters it seems that the process is reversible during the cycle heating–cooling–reheating (Fig. 5). One must also notice higher activation energies of the process for sample 3.

In Table 5 are listed the peak temperatures, the thermal effects and the mass variations obtained by means of TG/DTG/DTA analyses. The peak temperatures were measured on the curve where it was most obvious—DTG or DTA. Prior to the corrosion process, the samples were analysed by TG/DTG/DTA only in air, while after corrosion the samples were studied both in air and nitrogen.

The original samples presented a mass increase due to the oxidation processes of zinc and cooper [15]. As expected from the electrochemical tests, amongst the three samples, sample 1 has the lowest stability and started to get oxidised first at the lowest temperature.

Samples 2 and 3 have a similar behaviour in three main steps (Fig. 6).

After corrosion, sample 1 behaves in air similar to the uncorroded one but with a higher mass increase due to the destruction of passive layer from the surface. Samples 2 and 3 still behave similar when heated in air but the first oxidation step disappears (Fig. 7).

When heated in nitrogen the oxidation processes are covered by the decomposition of the formed corrosion products. This is proved also by the fact that the oxidation exothermic effects turn into decomposition endothermic effects. In fact, in all studied cases the last step had an endothermic effect.

All samples present mass losses. The highest is shown by sample 2—maybe due to the fact that the indium and its oxide are also volatile at high temperatures [16]. The most resistant sample to corrosion (sample 3—containing Ni) has the best behaviour after corrosion also from the thermal analysis point of view. This fact can be explained by the good passivation of the material when treated with the corrosive agent.

Table 4 Kinetic parameters obtained by means of DSC analyses on the studied alloys

| Sample	Heating rate/°C min^{-1}	ln(k_0)	E_a/kJ mol^{-1}	n
Sample 2 (heating)	5	244.21 ± 1.95	1220.27 ± 9.54	0.79 ± 0.001
	10	236.47 ± 2.34	1179.81 ± 11.47	1.17 ± 0.019
	15	264.98 ± 3.06	1316.91 ± 14.97	2.09 ± 0.028
Sample 2 (re-heating)	5	225.17 ± 1.96	1127.31 ± 9.58	0.58 ± 0.001
	10	280.08 ± 2.59	1393.59 ± 12.69	1.39 ± 0.018
	15	275.83 ± 3.15	1370.50 ± 15.44	2.21 ± 0.029
Sample 3 (heating)	5	428.28 ± 1.15	2119.61 ± 5.68	0.96 ± 0.004
	10	378.02 ± 1.18	1887.68 ± 5.83	1.39 ± 0.057
	15	356.92 ± 0.63	1781.73 ± 3.13	1.40 ± 0.032

Fig. 5 DSC heating–cooling–reheating cycle for sample 2
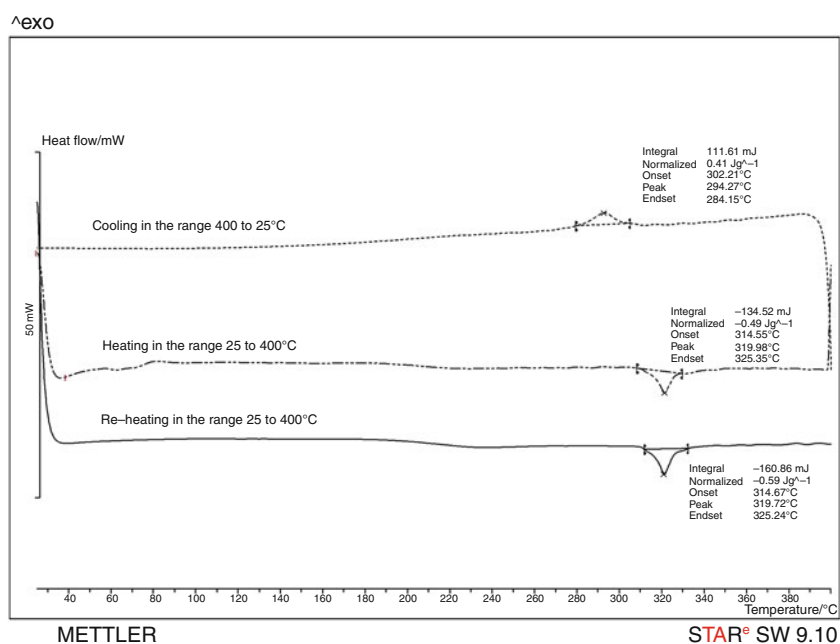
Table 5 TG/DTG/DTA analyses on the studied alloys

| Sample	T_1/°C Mass var./% DTA	T_2/°C Mass var./% DTA	T_3/°C Mass var./% DTA
Sample 1	–	[a]	907.2 (DTA) + 0.66 (endo)
Sample 1/corroded in air	–	[b]	906.31 (DTA) + 1.2 (endo)
Sample 1/corroded in N_2	–	807.81 (DTA) − (endo)	917.85 (DTA) − 3.24 (endo)
Sample 2	679.64 (DTG) + 0.61 (exo)	731.06 (DTG) + 0.49 (exo)	902.7 (DTG) + 1.14 (endo)
Sample 2/corroded in air	–	832.12 (DTG) + 0.74 (exo)	923.23 (DTG) + 0.93 (endo)
Sample 2/corroded in N_2	–	796.49 (DTA) − (endo)	879.32 (DTA) − 4.26 (endo)
Sample 3	667.67 (DTG) + 0.48 (exo)	814.96 (DTG) + 0.41 (exo)	866.85 (DTG) + 1.44 (exo)
Sample 3/corroded in air	–	747.09 (DTG) + 1.37 (exo)	–
Sample 3/corroded in N_2	–	–	834.59 (DTA) − 0.93 (endo)

[a] There is a slow mass increase in the range 463.9–1000 °C

[b] There is a slow mass increase in the range 590–1000 °C

Fig. 6 TG/DTG/DTA analyses for sample 2 before the corrosion process
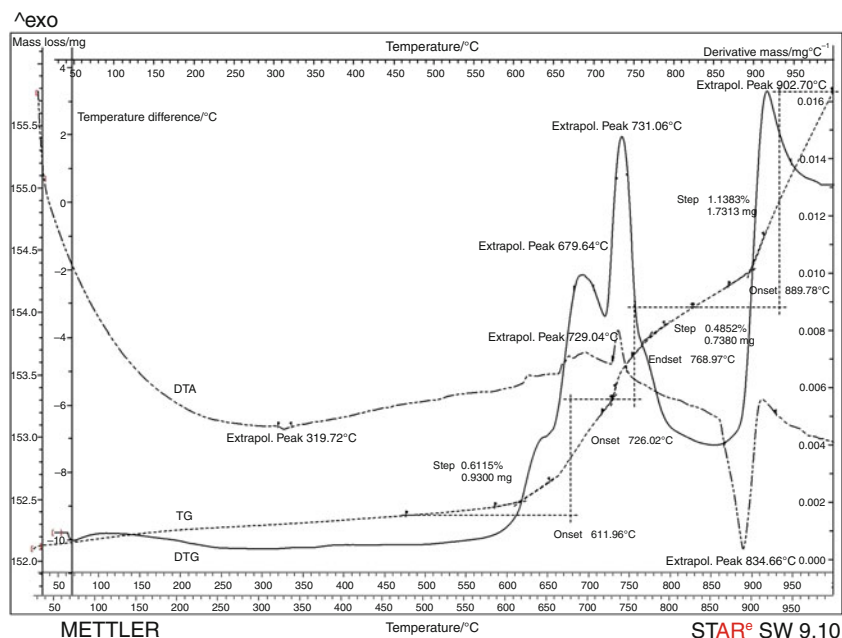
Fig. 7 TG/DTG/DTA analyses for sample 2 after the corrosion process
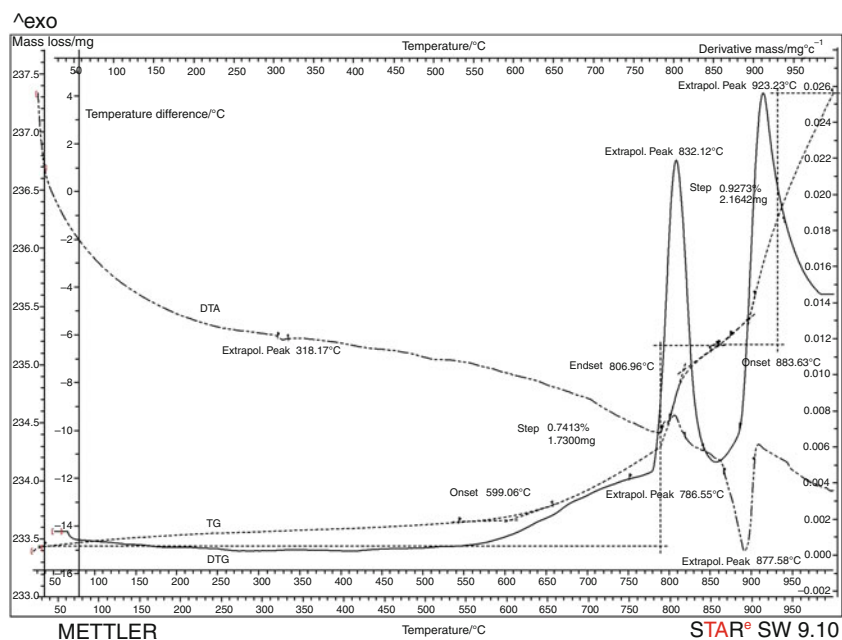
However, we must mention here that the phenomena occurring during the heating are very complex due to the superposition of two opposite processes—the oxidation of the metals contained by the alloys and the decomposition of the oxidation and corrosion products.

Conclusions

Electrochemical testing as an investigation method of ancient and historic metal has the potential to replace the subjective, visual assessment of degree of corrosion associated with the Oddy test [17] in the evaluation of material state of conservation.

The EIS results exhibited relative capacitive behaviour (good corrosion resistance) with phase angle close to -70° and relative large impedance values (order of 10^4 Ω cm^2) at low and medium frequencies, which are indicative of the formation of an oxide layer on these alloys after 1 h and 1 day of immersion in simulated acid rain. The EIS analysis has shown that the resistance of the oxide film formed on brass alloy samples increased with immersion time. Equivalent circuits were proposed to electrochemical behaviour of all brass alloys in simulated acid rain. EIS

technique requires minimal invasive procedures; i.e. neither the oxidation nor the reduction was forced to take place in the open circuit mode.

No effective protection against corrosion was achieved by all the samples, as the passive oxide film formed on the brass alloy cannot effectively isolate the alloy from the aggressive environment.

The thermal analysis performed in air gave information on the oxidising stability of the samples—process which has similarities with the corrosion in acid solution and can be correlated with the respective results. On the other hand, thermal analysis performed in nitrogen atmosphere on corroded samples showed the decomposition of the corrosion products.

One may say that the thermal analysis and electrochemical methods give complementary information on the corrosive resistance of metallic alloys but in order to elucidate these complex processes and to correlate the two methods further studies must to be carried out.

References

1. Mikhailovsky YN. Theoretical and engineering principles of atmospheric corrosion of metals. In: Ailor WH, editor. Atmospheric corrosion. New York: Wiley; 1982. p. 85–105.
2. van Grieken R, Janssens K, editors. Cultural heritage conservation and environmental impact assessement by non-distructive testing and micro-analysis. London: Taylor and Francis Group; 2005. p. 183–97.
3. Scott DA, Podany J, Considine BB, editors. Ancient and historic metals: conservation and scientific research. Los Angeles: Getty Conservation Institute; 1994. p. 119–51.
4. Melniciuc Puica N. On the ultrasound cleaning of the silver icons. Eur J Sci Theol. 2005;1(1):77–83.
5. Mareci D, Chelariu R, Rusu I, Melniciuc-Puica N, Sutiman D. Electrochemical behaviour of some religious artefacts in simulated acid rain. Eur J Sci Theol. 2010;6(3):57–70.
6. Assis SL, Wolynec S, Costa I. Corrosion characterization of titanium alloys by electrochemical techniques. Electrochim Acta. 2006;51:1815–9.
7. Raman V, Nagarajan S, Rajendran N. Electrochemical impedance spectroscopic characterisation of passive film formed over b Ti–29Nb–13Ta–4.6Zr alloy. Electrochem Commun. 2006;8: 1309–14.
8. Mareci D, Chelariu R, Gordin DM, Ungureanu G, Gloriant T. Comparative corrosion study of Ti–Ta alloys for dental applications. Acta Biomater. 2009;5:3625–39.
9. Mareci D, Sutiman D, Cailean A, Mirza-Rosca JC. Electrochemical characterization of some dental materials in accelerated environmental testing. Environ Eng Manag J. 2009;8:397–407.
10. Bujoreanu LG, Craus ML, Rusu I, Stanciu S, Sutiman D. On the α-phase preferred recrystallization in a Cu–Zn–Al based shape alloy. J Alloy Compd. 1998;278:190–3.
11. Magaino S. Corrosion rate of copper rotating-disk-electrode in simulated acid rain. Electrochim Acta. 1997;42(3):377–82.
12. Milosev I, Kosec T, Strehblow HH. XPS and EIS study of the passive film formed on orthopaedic Ti–6Al–7Nb alloy in Hank's physiological solution. Electrochim Acta. 2008;53:3547–58.
13. Ismail KM, El-Egamy SS, Abdelfatah M. Effects of Zn and Pb as alloying elements on the electrochemical behaviour of brass in borate solutions. J Appl Electrochem. 2001;31:663–70.
14. Borchardt HJ, Daniels FJ. The application of differential thermal analysis to the study of reaction kinetics. Am Chem Soc. 1957; 79:41–6.
15. Rusu I, Craus ML, Sutiman D, Rusu A. On the possible formation of Aurivillius phases in the oxide system Bi_2O_3–ZnO–Nb_2O_5. J Serb Chem Soc. 2004;69(1):53–8.
16. Rusu I, Craus ML. Preparation and IR-spectroscopic characterisation of Cd_2InNbO_6 perovskite oxide. J Optoelectron Adv Mater. 2006;8(5):1884–8.
17. Moussa L. Nanoscience and nanotechnology applied to art conservation: improved oddy test using silver nanoparticle sensor. Pittsburgh: The Carnegie Mellon University; 2007. p. 6–7.